https://doi.org/10.7735/ksmte.2026.35.2.96

J. Korean Soc. Manuf. Technol. Eng.
ISSN 2508-5107(Online)

Check for updates

Experimental Characterization and Regression Modeling of Arc Height and Surface Roughness in Shot Peening

Hyun-Jeong Kang[a], Su-Bean Park[b], Su-Jin Kim[a,b,*]

[a] Department of Aerospace & Technology Management, Gyeongsang National University
[b] School of Mechanical and Aerospace Engineering, Gyeongsang National University

ARTICLE INFO

Article history:

Received	17	December	2025
Revised	15	January	2026
Accepted	19	January	2026

Keywords:
Shot peening
Arc height
Surface roughness
Regression modeling

ABSTRACT

The process of shot peening was modeled experimentally in terms of Almen arc height and the roughness of the treated surface using a multivariate regression framework. Experiments were conducted with controlled variations in the feed rate, orientation and position of the workpiece, and the resulting arc heights and surface roughness values were used to develop the models. The arc height model demonstrated strong predictive capability, yielding an R^2 of 0.906 (modeling dataset) and 0.615 (independent validation dataset). However, surface roughness exhibited more complex variability due to localized material responses and random interactions; although statistically significant, the roughness model demonstrated moderate predictive accuracy. These results highlight that arc height can be estimated reliably from global process descriptors, whereas roughness prediction requires additional micro-scale information. The proposed approach provides an interpretable foundation for process optimization and supports the integration of data-driven enhancements for future shot peening control systems.

1. Introduction

Shot peening is a surface enhancement technique that introduces compressive residual stress by bombarding a metallic surface with high-velocity spherical media. This process suppresses crack initiation and propagation, ultimately improving fatigue life[1,2]. For lightweight aerospace and automotive components, shot peening is widely applied to mitigate fatigue degradation while maintaining structural integrity. Oh S.H. has shown that re-peening can recover relaxed compressive stress and extend fatigue life in aluminum alloys such as Al7075-T6[3], and that shot peening also contributes to corrosion resistance, particularly in titanium alloys used for biomedical implants[4].

The arc height obtained from Almen strips has long been used as an index for shot peening intensity. The saturation curve method[5] remains the industrial standard for defining optimal peening intensity. Recent research has shown that roughness and subsurface deformation depend strongly on shot peening parameters, including exposure time, shot velocity, impact energy, and feed rate. Studies examining the combined effect of residual stress and roughness have shown that both properties influence high-cycle and ultra-high-cycle fatigue behavior. For instance, severe shot peening can

* Corresponding author. Tel.: +82-55-772-1636
E-mail address: sujinkim@gnu.ac.kr (Su-Jin Kim).

introduce refined surface grains and enhance fatigue resistance in AW7075 alloys[6]. Fretting-fatigue studies on Al7075-T651 have shown that residual stress and roughness interact to determine fatigue limits[7]. Broader investigations into residual stress, cell size, and roughness across different parameter conditions further demonstrate that shot peening effects are highly sensitive to process configuration and geometry[8]. Additional work in related surface-modification fields, including studies on phase transformations and load-dependent behavior of austenitic stainless steels[9], reinforces the importance of understanding how energy input and boundary conditions alter both surface integrity and material response.

Despite these advances, experimental studies that simultaneously characterize both arc height and surface roughness under realistic industrial blast conditions remain limited. Much of the existing literature has concentrated on ideal normal-impact configurations, flat specimens, or single-variable analyses, leaving significant gaps in understanding how geometric orientation, position-dependent exposure, and feed-rate variation jointly affect peening outcomes. Furthermore, quantitative predictive models linking process variables, strip orientation, and positional effects to both arc height and roughness are scarce, and correlations between the two properties are often inferred theoretically rather than derived from controlled experiments. Furthermore, most prior work assumes normal impact conditions and uniform flat geometries, whereas real components frequently experience inclined impacts and position-dependent peening coverage. Studies addressing geometric orientation, position dependency, and multivariable predictive modeling are insufficient.

To address these gaps, this study experimentally evaluates the influence of process time, strip orientation (|nx|, |ny|), position (pz), and feed rate on both arc height and surface roughness using SAE J442 Type-A Almen strips. Moreover, multivariate regression models for arc height and surface roughness are developed to quantify the contribution of each parameter. The findings form a basis for optimizing the shot peening process and support the development of digital-twin-based peening design approaches for complex aerospace structures.

(a) Shot peening equipment

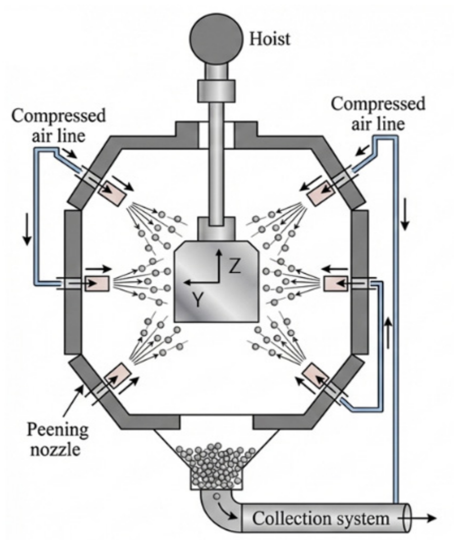

(b) Shot peening process schematic

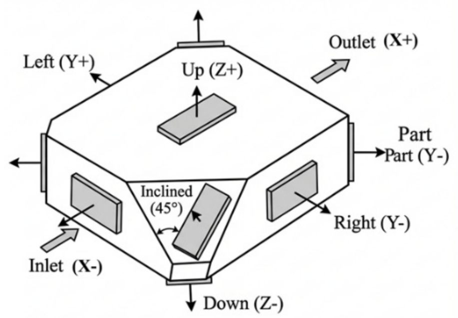

(c) Strip positioning and orientation

Fig. 1 Shot penning experimental methods

2. Experimental Methods

2.1 Shot peening procedure

SAE J442 Type-A Almen strips were used as specimens. All strips were cleaned and surface-prepared prior to peening to minimize external variability. Shot peening was performed using an automated system, as shown in Figure 1(a), equipped

Table 1 Process conditions for wheel-blast shot peening experiments

Parameter	Condition
Shot flow rate	600±50 lbs/min (fixed)
Stand-off distance	350 mm (fixed)
Impact angle	Horizontal, 30°, 45°
Feed rate (F)	0.3, 0.6, 1.2, 2.4 ±0.1 m/min
Peening duration	Inverse feed rate (1/F)

Wheel No.	Wheel rotational speed (±50 rpm)
1,3	1500
2,4	1500
5,6	1100
7,9	1400
8,10	1400
11,12	1100

with hard-cast steel shot (ASH230, 55–62 HRC). Figure 1 illustrates (b) the shot peening schematic and (c) the spatial orientation of Almen strip positioning. Strip placement followed a symmetric layout, including upper (Z+), lower (Z−), left (Y+), right (Y−), inlet (X−), outlet (X+), and inclined 45° regions to simulate realistic impact conditions on curved aerospace components.

Processing conditions were kept consistent throughout the experiments by maintaining the wheel rotational speed between 1200 and 1300 rpm, regulating the shot flow rate in pounds per minute, adjusting the impact angle to either horizontal, 30°, or 45°, and operating at feed rates of 0.3, 0.6, 1.2, and 2.4 m/min, while the shot peening duration was varied as the primary experimental parameter.

Table 1 summarizes the process conditions used in the wheel-blast shot peening experiments. All parameters except feed rate, strip orientation, and position were kept constant to isolate the effects of exposure time and geometric factors on arc height and surface roughness.

2.2 Measurement and analysis method

In the current wheel-blast configuration, the effective peening duration at a given surface location is inversely proportional to the feed rate. Accordingly, the inverse feed rate (1/F) was adopted as a representative parameter for local exposure time throughout this study.

Arc height was measured using a certified Almen gauge, as shown in Figure 2(a). The saturation curve was constructed

(a) Arc height

(b) Surface roughness

Fig. 2 Measurement methods

by plotting Arc height versus the inverse feed rate to determine the saturation point. For each experimental condition, five repeated measurements were conducted. The reported values represent the arithmetic mean of the repeated measurements.

Surface roughness (Ra, Rz) was measured using a stylus-type profilometer at three representative surface locations per strip, as shown in Figure 2(b). Surface roughness Ra obtained from nine measurements per condition, corresponding to three repeated measurements at three different surface locations on each Almen strip.

A regression analysis workflow was applied, beginning with data collection and followed by the selection of key variables, including |nx|, |ny|, pz^2, and feed-rate–related terms. The variables nx and ny represent the directional cosine components of the Almen strip normal vector relative to the wheel coordinate system, reflecting strip orientation. The parameter pz denotes the normalized vertical position of the strip relative to the wheel centerline, and pz^2 was used to capture symmetric positional effects. Tables 2 and 3 are the strip orientation and position used for modeling and verification. Transformed feed-rate terms such as $1/F^{0.25}$ and $1/F^2$ were introduced to account for the nonlinear accumulation of impact density and exposure time, as confirmed by

Table 2 Strip orientation and position for modeling

Strip #	nx	ny	nz	pz
1	0	-1	0	1
2	0	0	1	1
3	0	-1	0	1
4	1	0	0	0.5
5	-1	0	0	0.5
6	0	-1	0	0
7	-0.707	0	-0.707	-1
8	0	0	-1	-1
9	0.707	0	-0.707	-1
10	-1	0	0	0.3
11	1	0	0	0.3
12	0	1	0	1
13	0	1	0	1
14	-1	0	0	0.5
15	1	0	0	0.5
16	0	1	0	0

regression residual analysis. Multivariate regression was then performed, after which significance was evaluated using p-values and ANOVA. The resulting model was validated to confirm its reliability. These procedures enabled the development of predictive models for arc height and surface roughness.

3. Measurement Results

3.1 Arc height

Figure 3(a) illustrates the variation in arc height as a function of shot peening duration. The arc height increased rapidly during the early stage and approached saturation, consistent with typical saturation curve behavior. Arc height saturation was defined as the condition under which further reductions in feed rate resulted in less than a 5% increase in measured arc height. Based on this criterion, saturation was observed at feed rates below approximately 1.0 m/min.

This trend arises because compressive residual stress accumulates quickly at the beginning of peening but stabilizes once the surface layer reaches its plastic deformation capacity[1]. Additional peening beyond this point contributes minimally to arc height improvement, thus offering diminishing returns for fatigue enhancement.

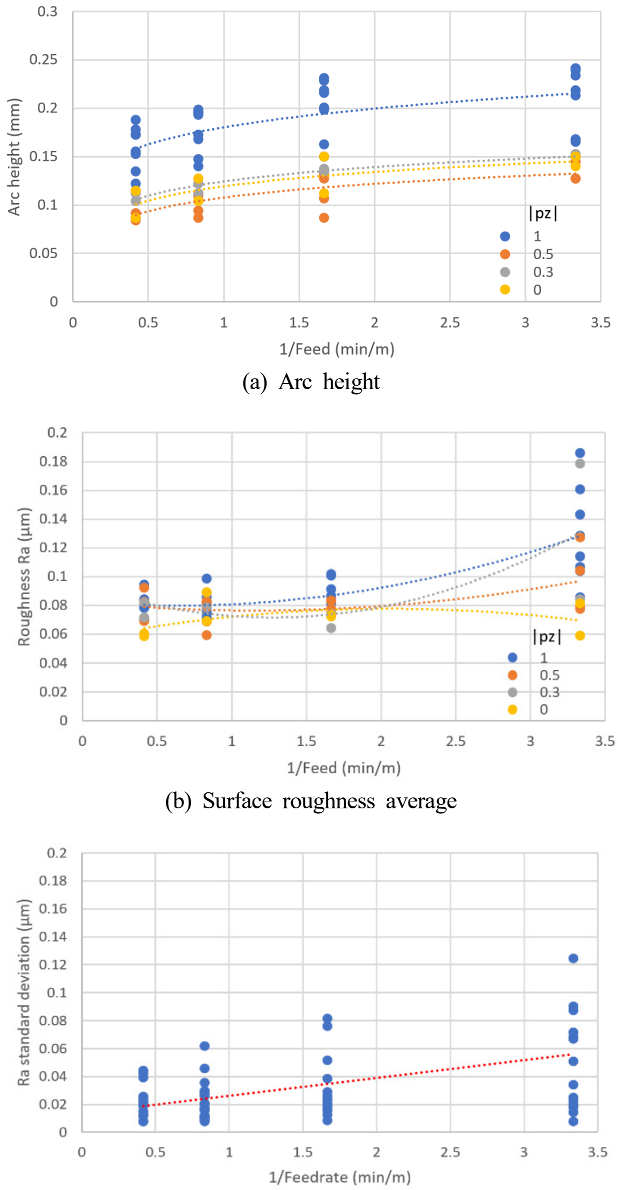

(a) Arc height

(b) Surface roughness average

(c) Ra standard deviation

Fig. 3 Measurement results

3.2 Surface roughness

Surface roughness showed weaker correlations with feed rate and arc height than the saturation trend observed for arc height. Figure 3(b) presents the variation of surface roughness Ra as a function of the inverse feed rate (1/F), plotted separately for different absolute position levels |pz|. Overall, Ra increases with increasing 1/F, indicating that lower feed rates (i.e., longer exposure time per unit length) produce rougher surfaces due to higher cumulative impact density. This trend is most pronounced for |pz| = 1, where Ra rises sharply at the highest 1/F values, reaching more than 0.18 μm.

The |pz| = 0.5 and |pz| = 0.3 cases show moderate roughness growth with increasing 1/F, although the slope is noticeably smaller than that of |pz| = 1. In contrast, the |pz| = 0 condition exhibits nearly constant Ra with minimal sensitivity to feed rate, indicating that peening exposure at the central position results in a more uniform impact distribution.

The separation between the curves demonstrates that surface roughness depends not only on feed rate but also strongly on spatial position relative to the wheel centerline. Positions with larger |pz|, corresponding to more inclined or peripheral impact conditions, experience greater surface deformation and thus higher roughness. This positional effect becomes more significant at low feed rates, where the cumulative impact intensity amplifies geometric sensitivity.

The average Ra was approximately 0.07 μm, and Rz was approximately 10 × Ra. Beyond the arc height saturation point, roughness continued to increase, reaching 0.72 μm for extended periods.

Figure 3(c) illustrates the standard deviation of surface roughness Ra obtained from nine measurements per condition, corresponding to three repeated measurements at three different surface locations on each Almen strip. The results show that the Ra standard deviation increases gradually with increasing inverse feed rate (1/F), indicating that surface roughness variability becomes more pronounced at lower feed rates. At higher 1/F values, prolonged peening exposure intensifies local plastic deformation and stochastic shot-surface interactions, resulting in greater spatial heterogeneity in surface topography.

At relatively high feed rates (low 1/F), the Ra standard deviation remains below approximately 0.03 μm, suggesting uniform surface modification with limited scatter. In contrast, at low feed rates (high 1/F), the standard deviation increases to values exceeding 0.08 μm in some cases, reflecting increased sensitivity to local impact conditions and cumulative shot overlap effects. This trend suggests that excessive peening duration not only increases the average surface roughness but also amplifies measurement dispersion, potentially affecting the consistency of surface quality.

These results demonstrate that although lower feed rates enhance peening intensity, they also introduce greater roughness variability. Therefore, from a process control perspective, both the mean Ra value and its standard deviation should be considered when defining optimal shot peening conditions, particularly for components requiring strict surface quality uniformity.

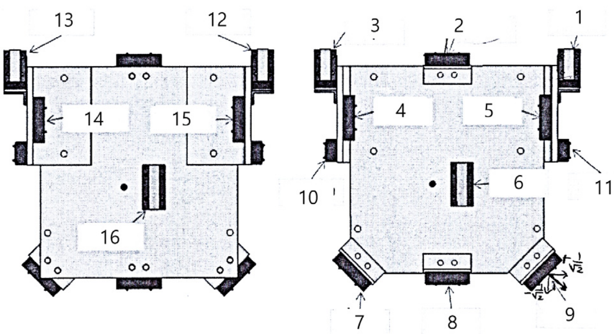

Fig. 4 Specimen geometry for regression model

4. Regression Analysis

The modeling and validation datasets were obtained from two independent experimental campaigns conducted on the same wheel-blast shot peening system but using different specimen geometries. The first specimen geometry, as shown in Figure 4 and Table 2, was used to construct the regression models for arc height and surface roughness. A second, geometrically distinct specimen, as shown in Figure 7, was used exclusively for model validation. This separation ensured that no identical geometric configurations or surface exposure conditions were shared between the modeling and validation datasets.

4.1 Arc height

Arc height was modeled using |nx|, |ny|, pz^2, and $1/F^{0.25}$ as independent variables. Figure 5(a) shows the predicted and measured arc height. The regression analysis yielded a strong correlation coefficient of 0.952, with R-squared values of 0.906 and 0.900, respectively, indicating excellent explanatory power. The standard error of 0.0142 confirmed the model's precision, and the ANOVA results, with an F-value of 142.62 and a p-value of 1.3×10^{-29}, demonstrated that the model was highly statistically significant. All independent variables were statistically significant ($p < 0.01$). pz^2 and $1/F^{0.25}$ exhibited the strongest influence. The final regression equation is equation (1).

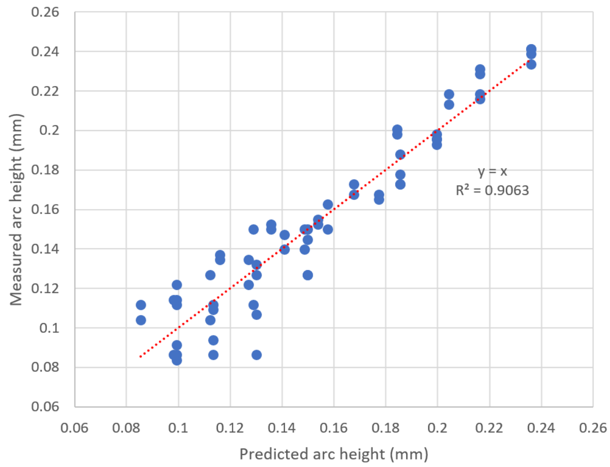

(a) Arc height

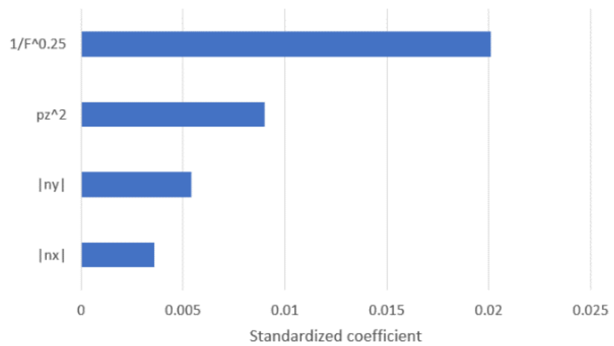

(b) Contribution of independent variables

Fig. 5 Multiple regression model arc height

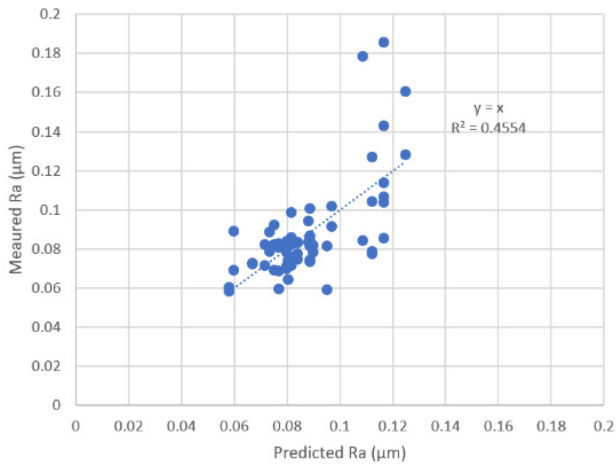

(a) Surface roughness

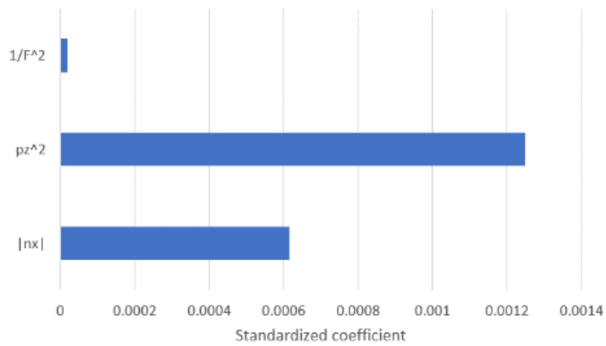

(b) Contribution of independent variables

Fig. 6 Multiple regression model of surface roughness

$$AH = -0.0343 + 0.0379\,|nx| + 0.0586\,|ny| + 0.0873(pz)^2 + 0.0920(1/F^{0.25}) \quad (1)$$

Figure 5(b) compares standardized coefficients, confirming the dominant effects of feed rate (F) and strip height (pz).

4.2 Surface roughness

Surface roughness was modeled using $|nx|$, pz^2, and $1/F^2$, yielding a correlation coefficient of 0.675, an R-squared of 0.455, and an adjusted R-squared of 0.428. Figure 6(a) shows the predicted and measured surface roughness. The standard error was 0.0191, and the ANOVA results (F-value = 16.7, p-value = 5.20 × 10^-8) confirmed that the model was statistically significant. Surface roughness shows greater variability than arc height, which explains the lower R^2 value. The regression model is equation (2)

$$Ra = 0.0576 + 0.0116\,|nx| + 0.0216(pz)^2 + 0.00338(1/F^2) \quad (2)$$

Figure 6(b) shows the standardized effect of each variable. Among the variables, pz^2 and $|n_x|$ were identified as highly influential predictors of Ra.

Table 2 Strip orientation and position for modeling

5. Verification Results and Discussion

The predictive performance of the proposed regression models was evaluated using arc height and surface roughness measurements from the shot peening verification experiments. By validating the regression models on a different specimen geometry (Figure 7 and Table 3) under the same equipment and process control conditions, the robustness and generalization capability of the proposed models with respect to geometric variation were systematically evaluated. Figures 8 and 9 summarize the comparison between model predictions and experimental observations, revealing the strengths and limitations of the developed analytical framework.

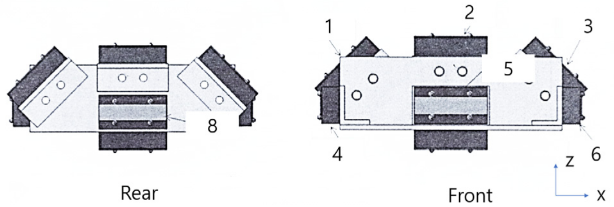

Fig. 7 Specimen geometry for verification experiment

Table 3 Strip orientation and position for verification

Strip #	nx	ny	nz	pz
1	-0.707	0	0.707	0.7
2	0	0	1	0.8
3	0.707	0	0.707	0.7
4	-1	0	0	0.2
5	0	-1	0	0.2
6	1	0	0	0.2
8	0	1	0	0.2

5.1 Arc height

Figure 8(a) presents the relationship between the predicted and measured arc heights for the validation dataset. The data points follow a clear upward trend, and the fitted line exhibits an R-square value of 0.615, indicating that the model captures a substantial portion of the physical variation in arc height, even under unseen processing conditions. Although the scatter increases at higher arc heights, the slope of the regression line approaches unity, suggesting that the model maintains consistent proportionality between predictions and measurements. This level of agreement confirms that the regression formulation, based on feed rate, impact momentum, and surface loading terms, can reliably approximate arc height generation in practical operational windows.

To further examine model behavior under changing feed rate conditions, Figure 8(b) compares the predicted and experimental arc heights as a function of 1/F. Both curves exhibit the expected trend of increasing arc height at lower feed rates, reflecting longer exposure times and greater cumulative energy imparted to the surface. The predicted values remain slightly higher than the experimental measurements across the full range, implying a mild systematic overestimation. Despite this offset, the parallel nature of the two curves demonstrates that the model correctly reproduces the functional dependence on feed rate and is suitable for parametric process optimization.

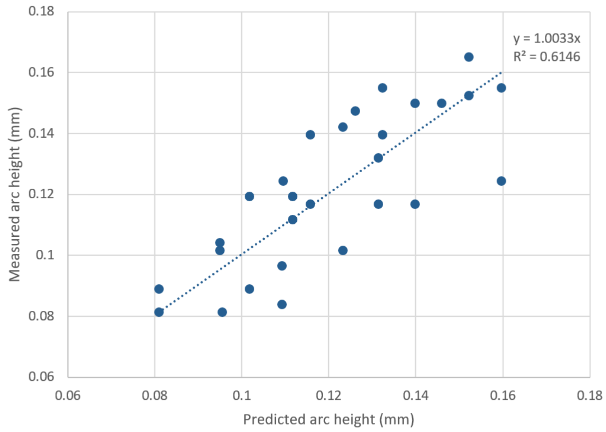

(a) Verification experiment

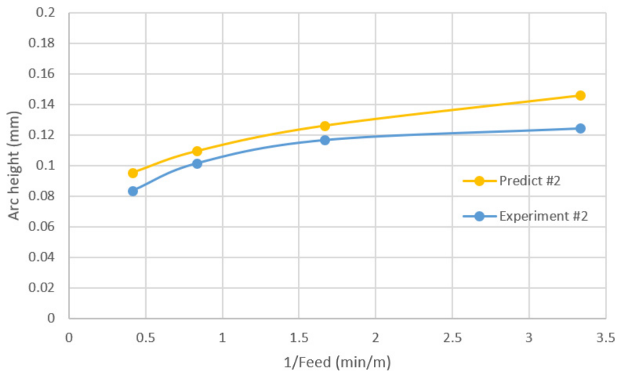

(b) Predicted and experimented arc height of strip #2

Fig. 8 Relationship between predicted and measured arc heights

5.2 Surface roughness

Figure 9(a) illustrates the predictive performance for surface roughness Ra, using the model constructed from |nx|, pz^2, and $1/F^2$. The distribution of data points exhibits a moderate positive correlation, consistent with the reported quantified R^2 value of 0.455. The surface roughness regression model's predictive capability is limited compared with that of the arc height model. Therefore, the roughness model should be interpreted as a trend-level estimator rather than a high-precision predictive tool. In practical applications, the model is suitable for identifying dominant process tendencies and relative parameter sensitivity, while local surface effects and stochastic shot-surface interactions may cause deviations in absolute Ra values.

To assess feed-rate dependency in surface roughness more explicitly, Figure 9(b) compares predicted and measured roughness values across the same 1/F range. The experimental roughness varies only slightly with feed rate, whereas the

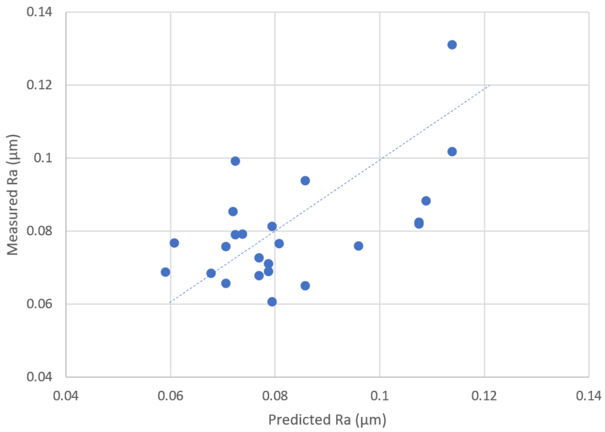

(a) Verification experiment

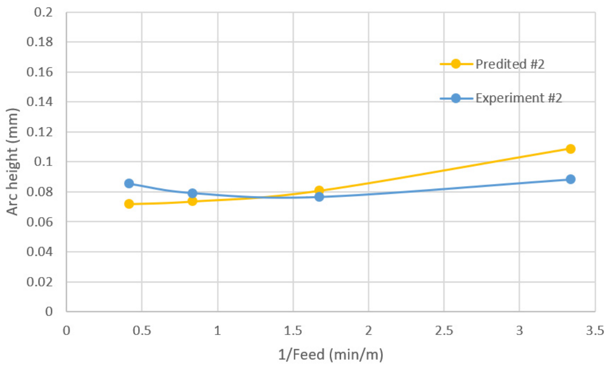

(b) Predicted and experimented Ra of strip #2

Fig. 9 Relationship between predicted and measured surface roughness

model predicts a more pronounced upward trend at lower feed values. This difference suggests that the influence of feed-related exposure time is weaker in practice than the model assumes.

Overall, the comparative results demonstrate that the arc height model offers robust predictive capability across both training and validation datasets, with clear physical consistency and strong correlation. The roughness model, while statistically significant, shows greater variability and could be refined. These observations confirm that the developed modeling framework is effective for predicting arc height behavior; however, it requires further enhancement for applications where surface finish is the dominant quality requirement.

6. Conclusion

This study developed and validated regression-based predictive models for arc height and surface roughness generated during shot peening under controlled wheel-blast processing conditions. The modeling approach incorporated physically meaningful variables, including normal impact momentum, feed-rate-dependent exposure terms, and surface-loading metrics derived from process kinematics. Experimental data demonstrated that the arc height model achieved strong predictive capability, with R-squared values of 0.906 for the modeling dataset and 0.615 for the independent validation dataset. The model successfully reproduced the functional dependence on feed rate and impact momentum, and its predictions remained consistent across the full range of operating conditions evaluated.

Surface roughness exhibited more complex behavior due to localized deformation and the inherent variability in shot-surface interactions. Although the roughness model was statistically significant and accurately captured overall trends, its predictive accuracy was lower, with a moderate correlation coefficient and noticeable discrepancies at low feed conditions.

Overall, the results confirm that the proposed regression framework provides a reliable and interpretable tool for predicting arc height formation in shot peening processes, offering a baseline methodology for roughness estimation. Future work will incorporate machine-learning-based parameter augmentation to enhance predictive fidelity and enable fully integrated process optimization.

Acknowledgement

This work was supported in part by the Glocal University 30 Project Fund of Gyeongsang National University.

References

[1] Cheng, Y., Wang, Y., Lin, J., Xu, S., Zhang, P., 2023, Research Status of the Influence of Machining Processes and Surface Modification Technology on the Surface Integrity of Bearing Steel Materials, Int. J. Adv. Manuf. Technol., 125 2897-2923, https://doi.org/10.1007/s00170-023-10960-x.

[2] Farrahi, G. H., Lebrijn, J. L., Couratin, D., 1995, Effect of Shot Peening on Residual Stress and Fatigue Life of a Spring Steel,

Fatigue Fract. Eng. Mater. Struct., 18:2 211-220, https://doi.org/10.1111/j.1460-2695.1995.tb00156.x.

[3] Oh, S. H., Lee, Y. S., Cheong, S. K., 2016, Effects of Re-Peening on the Compressive Residual Stress and Fatigue Life of Al7075-T6, J. Korean Soc. Manuf. Technol. Eng., 25:4 253-257, https://doi.org/10.7735/ksmte.2016.25.4.253.

[4] Oh, S. H., Cheong, S. K., Shin, K. H., 2018, Corrosion Resistance of Shot Peened Ti-6Al-4V by Additional Surface Treatment, J. Korean Soc. Manuf. Technol. Eng., 27:2 120-124, http://doi.org/10.7735/ksmte.2018.27.2.120.

[5] Kirk, D., 2002, Curve Fitting for Shot Peening Data Analysis, Shot Peener, 16:1 6-11, <https://www.shotpeener.com/library/pdf/2002139.pdf>.

[6] Trško, L., Guagliano, M., Bokůvka, O., Nový, F., Jambor, M., Florková , Z., 2017, Influence of Severe Shot Peening on the Surface State and Ultra-High-Cycle Fatigue Behavior of an AW 7075 Aluminum Alloy, J. Mater. Eng. Perform, 26 2784-2797, https://doi.org/10.1007/s11665-017-2692-9.

[7] Martín, V., Vázquez, J., Navarro, C., Domínguez, J., 2020, Effect of Shot Peening Residual Stresses and Surface Roughness on Fretting Fatigue Strength of Al 7075-T651, Tribol. Int., 142 106004, https://doi.org/10.1016/j.triboint .2019. 106004.

[8] Lin, Q., Liu, H., Zhu, C., Chen, D., Zhou, S., 2020, Effects of Different Shot Peening Parameters on Residual Stress, Surface Roughness and Cell Size, Surf. Coat. Technol., 398 126054, https://doi.org/10.1016/j.surfcoat.2020.126054.

[9] Beck, T., Smaga, M., Antonyuk, S., Eifler, D., Müller R., Urbassek, H. M., Zhu, T., 2023, Influence of Manufacturing and Load Conditions on the Phase Transformation and Fatigue of Austenitic Stainless Steels, In: Component Surfaces: Manufacturing–Morphology–Property Relationships, Springer, Switzerland, 257-288, https://doi.org/10.1007/978-3-031-35 575-2_11.

Hyun-Jeong Kang
Student in the Department of Aerospace & Technology Management, Gyeongsang National University. Her research interests include quality management.
E-mail: kkhj2635@naver.com

Su-Been Park
Student in the School of Mechanical and Aerospace Engineering, Gyeongsang National University. Her research interests include CNC machining and production quality.
E-mail: subean0607@gnu.ac.kr

Su-Jin Kim
Professor in the School of Mechanical and Aerospace Engineering, Gyeongsang National University. His research interests include CAM and CNC machining.
E-mail: sujinkim@gnu.ac.kr